Physical effects underlying the transition from primitive to modern cell membranes

Itay Budin[a,b] and Jack W. Szostak[a,b,1]

[a]Howard Hughes Medical Institute, and [b]Department of Molecular Biology, and the Center for Computational and Integrative Biology, Massachusetts General Hospital, Boston, MA 02114

Edited by Gerald F. Joyce, The Scripps Research Institute, La Jolla, CA, and approved February 17, 2011 (received for review January 10, 2011)

To understand the emergence of Darwinian evolution, it is necessary to identify physical mechanisms that enabled primitive cells to compete with one another. Whereas all modern cell membranes are composed primarily of diacyl or dialkyl glycerol phospholipids, the first cell membranes are thought to have self-assembled from simple, single-chain lipids synthesized in the environment. We asked what selective advantage could have driven the transition from primitive to modern membranes, especially during early stages characterized by low levels of membrane phospholipid. Here we demonstrate that surprisingly low levels of phospholipids can drive protocell membrane growth during competition for single-chain lipids. Growth results from the decreasing fatty acid efflux from membranes with increasing phospholipid content. The ability to synthesize phospholipids from single-chain substrates would have therefore been highly advantageous for early cells competing for a limited supply of lipids. We show that the resulting increase in membrane phospholipid content would have led to a cascade of new selective pressures for the evolution of metabolic and transport machinery to overcome the reduced membrane permeability of diacyl lipid membranes. The evolution of phospholipid membranes could thus have been a deterministic outcome of intrinsic physical processes and a key driving force for early cellular evolution.

origin of life | ribozymes | coevolution

The first cell membranes are likely to have formed from simple, single-chain lipids such as short-chain fatty acids and their derivatives that were present in the prebiotic environment (1, 2). Membranes composed of such amphiphiles are permeable to polar nutrients such as nucleotides (3) and feature the dynamic properties necessary for spontaneous growth and division (2, 4). The high permeability of fatty-acid-based membranes is consistent with a heterotrophic model for early cells, in which chemical building blocks are synthesized in the environment and passively diffuse across the cell membrane to participate in replication. All modern cells synthesize phospholipids (or sulfolipids in rare exceptions; refs. 5 and 6) with two hydrophobic chains as their primary membrane lipids. Phospholipid membranes prevent the rapid permeation of ions and polar molecules, allowing modern cells to retain internally synthesized metabolites and to control all import and export. The evolution of phospholipid membranes must have therefore mirrored the emergence of metabolic and transport machinery during early cellular evolution.

This transition from single-chain lipids to phospholipids had to be gradual, both to allow for the coevolution of metabolic and transport machinery and because of the initial inefficiency of nascent catalysts (e.g., ribozymes). Hence, the selective advantage associated with phospholipid synthesis had to apply to small differences in phospholipid content in order to drive this transition. What selective advantage could be conferred by the low levels of phospholipid that must have been present at the beginning of this process? Our laboratory has previously demonstrated that populations of fatty acid vesicles, representing primitive cellular compartments (protocells), are able to compete directly with each other via the exchange of fatty acid monomers (7). These exchange processes allow some vesicles to grow at the expense of others, e.g., RNA-induced osmotic swelling causes vesicles to grow by incorporating fatty acids from empty vesicles. Here we asked whether low levels of phospholipids, potentially synthesized by genomically encoded catalysts (e.g., ribozymes), could also drive competitive growth and therefore provide a clear selective pressure for the evolution of modern cell membranes. We were motivated by previous experiments suggesting that phospholipid-containing micelles can alter the fatty acid equilibrium between vesicles and micelles (8) and that pure phosphatidylcholine vesicles disrupt neighboring oleate vesicles (9).

Results

Phospholipid-Driven Growth of Fatty Acid Vesicles. To address the hypothesis that phospholipids could drive competition between protocells, we asked whether mixed fatty acid/phospholipid vesicles grow upon mixing with pure fatty acid vesicles. To monitor surface area change, we measured the Förster resonance energy transfer (FRET) between donors and acceptor fluorophores included at a fixed initial concentration in the bilayer. This assay quantitatively measures surface area by relating the decrease (or increase) in FRET to a change in fluorophore concentration (2, 7). We first asked whether 100 nm oleate vesicles containing 10 mol % di-oleoyl-phosphatidic acid (DOPA) grow upon mixing with 1 equivalent of pure oleate vesicles (Fig. 1*A*). After mixing, an approximate 16% increase in the surface area of the phospholipid-containing vesicles was observed ($k = 0.1\ s^{-1}$). Mixing with either buffer or vesicles of the same composition did not lead to growth. We also observed the corresponding shrinkage of pure oleate vesicles upon mixing with vesicles containing 10 mol % DOPA (Fig. 1*B*), but not upon mixing with buffer or with additional oleate vesicles.

The emergence of a catalytically functional polymer from a population of random sequences would have been a rare stochastic event. Within a population of protocells, the first cell containing a phospholipid synthase catalyst would have been surrounded by a vast excess of protocells that could not synthesize phospholipids. We therefore considered the effect of the ratio of phospholipid-containing vesicles to pure fatty acid vesicles on the magnitude of the observed growth. We found that the amount of growth increased continuously as the ratio of fatty acid donor vesicles to phospholipid-containing acceptor vesicles increased (Fig. 1*C*). Indeed, the extent of growth appears to be limited only by the eventual dilution of initial phospholipid content. As a result, early phospholipid synthesizing cells would be expected to grow

Author contributions: I.B. and J.W.S. designed research; I.B. performed research; I.B. and J.W.S. analyzed data; and I.B. and J.W.S. wrote the paper.

The authors declare no conflict of interest.

This article is a PNAS Direct Submission.

Freely available online through the PNAS open access option.

[1]To whom correspondence should be addressed. E-mail: szostak@molbio.mgh.harvard.edu.

This article contains supporting information online at www.pnas.org/lookup/suppl/doi:10.1073/pnas.1100498108/-/DCSupplemental.

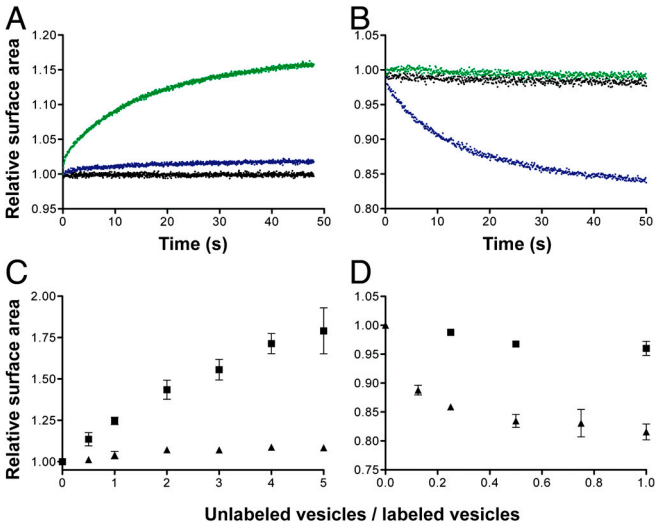

Fig. 1. Phospholipids drive competition between fatty acid vesicles. (*A* and *B*) Competition between vesicles was monitored by a FRET-based real-time surface area assay. Growth of FRET-labeled 90:10 oleate:DOPA vesicles (*A*) and shrinkage of FRET-dye labeled oleate vesicles (*B*) when mixed 1:1 with buffer (black), unlabeled oleate vesicles (green), or unlabeled 90:10 oleate:DOPA vesicles (blue). (*C* and *D*) The dependence of vesicle growth or shrinkage on vesicle stoichiometry. Final growth after equilibrium of FRET-labeled 90:10 oleate:DOPA vesicles (*C*) and shrinkage of FRET-labeled oleate vesicles (*D*) when mixed with varying amounts of unlabeled oleate (■) or unlabeled 90:10 oleate:DOPA (▲) vesicles. Error bars indicate SEM ($N = 3$).

continuously, at the expense of neighboring vesicles, at a rate controlled by the rate at which they could synthesize phospholipid.

We next asked whether phospholipid-driven growth could facilitate vesicle division, as has been demonstrated for the growth of large multilamellar vesicles following fatty acid micelle addition (4). We prepared large (approximately 4 μ) multilamellar oleate vesicles containing 10 mol % DOPA and an encapsulated soluble dye (Fig. 2*A*). Upon mixing with a large excess of unlabelled oleate vesicles, rapid growth was observed (Fig. 2*B*). Remarkably, growth proceeded by the same pathway as previously observed (4) following the rapid addition of excess fatty acid micelles: the extrusion of a thin tubular tail from the vesicle, followed by the transformation of the original spherical vesicle into a long, narrow filamentous vesicle (Fig. 3*D*). The cause of this shape change is the lag between surface area growth and volume growth, which is osmotically limited by the slowly permeating buffer in the medium (*SI Appendix*, Fig. S1). When a mild shear force was applied to these filamentous structures by gentle agitation, efficient vesicle division was observed (Fig. 3*C*). This pathway allows for spontaneous protocell division without the need for preexisting cellular machinery but is inaccessible by osmotically driven competition, which leads to the growth of swollen and therefore spherical vesicles. We obtained similar results in experiments using a more prebiotically plausible lipid mixture of 2:1 decanoic acid: decanol and 10 mol % of didecanoyl-phosphatidic acid (DDPA) (*SI Appendix*, Fig. S2). This mixture of short saturated single-chain amphiphiles mimics the major products of the abiotic Fischer–Tropsch–Type synthesis (10) and lipids extracted from the Murchison meteorite (11).

Mechanism of Competitive Growth. Monomer desorption is the rate-limiting step in the exchange of fatty acids between vesicles (12). We therefore hypothesized that phospholipids drive competitive growth by reducing the efflux of fatty acid, leaving the membrane while keeping the influx of fatty acids unchanged. In principle, two effects could decrease the flux of fatty acids desorbing from a membrane: first, a decreased fatty acid off-rate in the presence of phospholipids and, second, a decrease in the net efflux from the membrane due to the reduced fraction of the membrane surface area occupied by fatty acids.

To ask whether phospholipids decrease fatty acid off-rates, we measured oleate desorption rates from mixed bilayer membranes using a stopped-flow fluorescence assay (13). We measured fatty acid desorption rates by monitoring the drop in fluorescence over time of a pH-sensitive dye encapsulated within phospholipid reporter vesicles. The decrease in fluorescence is caused by the adsorption of fatty acids into the reporter vesicle membrane, followed by flip-flop across the bilayer in a protonated form, and subsequent proton release on the interior face of the reporter vesicle (*SI Appendix*, Fig. S3). We found that oleate desorption was progressively slowed by increasing DOPA content in the donor vesicles, so that desorption from a pure fatty acid bilayer was threefold faster than desorption from an almost pure phospholipid bilayer (Fig. 3*A*). This latter rate is consistent with previously measured (13) oleate desorption rates from phospholipid bilayers. Assuming that adsorption is unaffected, reducing the

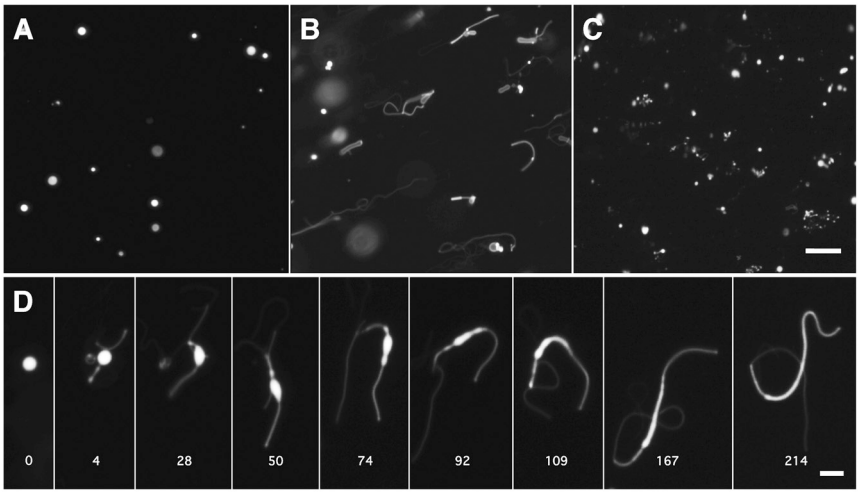

Fig. 2. Phospholipid-driven growth leads to a filamentous shape transition and vesicle division. (*A*) Large, multilamellar 90:10 oleate:DOPA vesicles, labeled with an encapsulated soluble dye, are initially spherical. (*B*) Upon mixing with a 100-fold excess of unlabeled oleate vesicles, the mixed vesicles rapidly grow into long, filamentous vesicles. (*C*) The fragile filamentous vesicles then readily divide into small daughter vesicles upon the application of gentle shear forces (see *Methods*). (Scale bar: 30 μm.) (*D*) Time course showing the shape transformation of a labeled 90:10 oleate:DOPA vesicle upon addition of unlabeled oleate vesicles. Time in seconds. (Scale bar: 5 μm.)

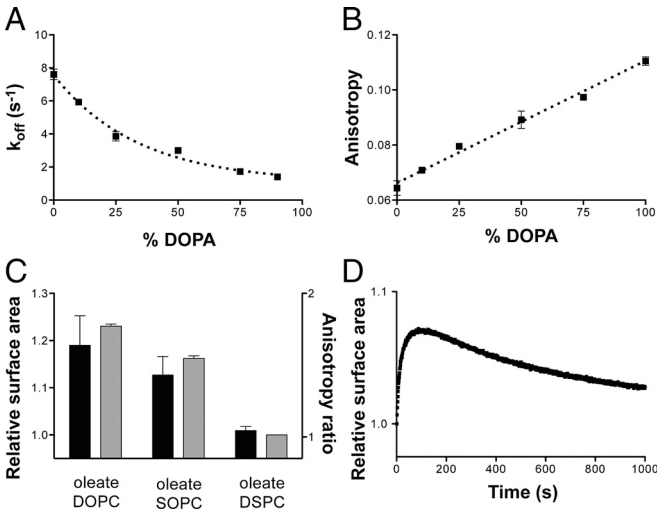

Fig. 3. Mechanisms of phospholipid-driven growth. (*A*) The desorption rate of oleate in mixed oleate/DOPA vesicles as a function of DOPA content. Increasing phospholipid content slows oleate desorption, leading to growth of phospholipid-enriched vesicles. (*B*) The steady-state anisotropy of DPH in oleate/DOPA vesicles as a function of DOPA content. Bilayer packing order increases linearly with increasing fraction of the diacyl lipid. Dashed line indicates linear regression fit, $R^2 = 0.98$. (*C*) The extent of growth of FRET labeled 90:10 oleate:DSPC vesicles when mixed 1:1 with the given 90:10 vesicle composition (black bars, left axis) correlates with the ratio of the membrane fluidity between oleate/DSPC bilayers and those of the given composition as measured by DPH anisotropy (gray bars, right axis). DOPC, di-oleoyl-phosphocholine (C18:1); SOPC, 1-stearoyl-2-oleoyl-phosphocholine (C18:0/C18:1). (*D*) Growth of FRET-labeled 90:10 oleate:NA vesicles when mixed 1:1 with unlabeled oleate vesicles. Growth proceeds in the first 60 s, followed by a slow relaxation due to the equilibration of the slowly exchanging NA fraction. Error bars indicate SEM ($N = 3$).

off-rate of fatty acids would then drive both growth of the phospholipid-containing vesicles and shrinkage of the pure fatty acid vesicles (*SI Appendix*). The effect of phospholipid on the oleate desorption rate is sufficient to explain the magnitude of growth that we observed in competition experiments: 10 mol % DOPA inhibited oleate desorption by 22%, corresponding to an expected surface area change of 14% at equilibrium (experimental, 16%) in 1:1 competition experiments (e.g., Fig. 1*A*). The free energy values for oleate dissociation derived from these rates were linearly dependent on phospholipid content (*SI Appendix*, Fig. S4), indicating that a noncooperative phospholipid-fatty-acid interaction was responsible for the observed effects.

To characterize the structural basis for the phospholipid-driven decrease in desorption rate, we measured the effectiveness of a variety of phospholipids. The oleate desorption rate was mildly dependent on phospholipid head group structure (*SI Appendix*, Fig. S5*A*), consistent with the potential of the head group to hydrogen bond with fatty acids in the bilayer (14, 15). We observed a stronger effect by varying the acyl chain composition of the phospholipid; saturated acyl chains inhibited desorption more than phospholipids with unsaturated or branched chains (*SI Appendix*, Fig. S5*B*). Saturated acyl chains, lacking *cis* double bonds, permit increased interacyl chain van der Waals interactions and thus form more ordered membranes (16). This effect led us to hypothesize that diacyl lipids slow fatty acid desorption by increasing the acyl chain order in the bilayer. Because more closely packed acyl chains are expected to have a higher affinity for each other, an increase in bilayer order would slow monomer desorption, as has been observed for the desorption of cholesterol (17) and phospholipids (18). To test this hypothesis, we measured the steady-state fluorescence anisotropy of the fluorophore 1,6-diphenyl-1,3,5-hexatriene (DPH), a reporter of the microviscosity of the bilayer interior (19). As expected, oleate membranes exhibited significantly lower anisotropy than DOPA membranes, indicating that monoacyl membranes are less ordered and more fluid than their corresponding diacyl membranes (Fig. 3*B*). The anisotropy of mixed membranes was linearly dependent on the diacyl lipid content, an observation consistent with the desorption rates in mixed membranes. The anisotropy of mixed membranes containing acyl chain analogues (*SI Appendix*, Fig. S6) also correlated with the rate of oleate desorption in these mixtures (*SI Appendix*, Fig. S5*B*). To confirm that lower fluidity can independently drive growth, we measured the change in surface area of oleate vesicles containing 10 mol % of di-stearoyl-phosphocholine (DSPC), a saturated chain phospholipid, after mixing with oleate vesicles containing equal amounts of unsaturated PCs (Fig. 3*C*, black bars). The DSPC-containing vesicles grew at the expense of vesicles containing unsaturated PCs, with the magnitude of growth in agreement with the ratio of their fluidity measurements via DPH anisotropy (Fig. 3*C*, gray bars). Because both saturated and unsaturated PCs are essentially insoluble in water, the growth of the membranes containing DSPC cannot be due to a dilution effect, but must instead reflect the increased order that the phospholipids introduce to the fatty acid bilayer.

In addition to the desorption effect described above, competition could also be driven by the entropically favored dilution of the insoluble phospholipid fraction in the fatty acid membrane. Mechanistically, this mode of growth occurs because only the fraction of the vesicle surface area composed of fatty acids can contribute to monomer efflux, whereas the entire surface area permits fatty acid influx, leading to a net influx (growth) in the presence of pure fatty acid vesicles. To test this mechanism independently of off-rate effects, we screened for lipids with low solubility that do not alter the fluidity of oleate membranes. Nervonic acid (NA), a 24 carbon unsaturated fatty acid, is stable in oleate vesicles as a minor fraction without affecting bilayer fluidity (*SI Appendix*, Fig. S7) but has a longer residence time than oleate due to its longer chain length. When oleate vesicles containing 10 mol % NA were mixed with pure oleate vesicle, we observed an initial period of growth, as in the case of the phospholipid-containing vesicles. However, this growth phase was followed by a slow loss of the added surface area as the NA equilibrated between the two vesicle populations. Because the off-rate of a lipid from a bilayer is dependent on the number of carbon atoms in its acyl chain(s), a very long chain monoacyl lipid that remains in the bilayer indefinitely would be sufficient to drive growth. However, there is no prebiotic route to such species, whereas diacyl lipid synthesis is a simple chemical means of producing insoluble lipids via the linkage of two, short acyl chains (20, 21).

We have identified two distinct mechanisms by which phospholipids can drive competitive growth at the expense of pure fatty acid vesicles. Because both the rate of fatty acid desorption (Fig. 3*A*) and the surface fraction of insoluble phospholipid scale throughout the binary mixture range (0–100 mol %), competition for fatty acids and related molecules should be driven by any difference in phospholipid content between vesicles. Consistent with this prediction, we observed growth of oleate vesicles containing 75 mol % DOPA upon mixing with vesicles containing 25 mol % DOPA (*SI Appendix*, Fig. S8). Early cells that were capable of synthesizing more phospholipid could therefore have grown at the expense of other cells that synthesized less phospholipid, which would have led to an evolutionary arms race (22) driving increasing diacyl lipid content in early cell membranes.

Effect of Increasing Phospholipid Content on Membrane Permeability. What would have been the consequences of such an inexorable transition from monoacyl to diacyl lipid membranes? If high membrane permeability was necessary for early heterotrophic cells to take in chemical building blocks from the environment,

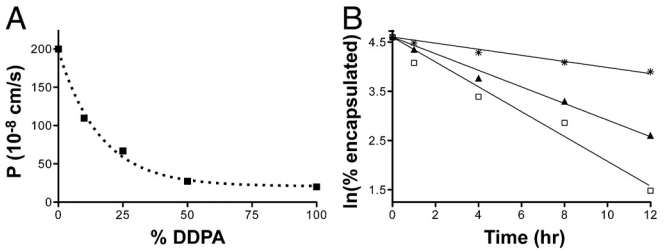

Fig. 4. Phospholipids inhibit solute permeation through fatty-acid-based membranes. (*A*) Permeability of C10 membranes (4:1:1 DA:DOH:GMD) to ribose as a function of DDPA content as measured by a stopped-flow relaxation assay. (*B*) Leakage of encapsulated ImpdA from C10 vesicles as measured by scintillation counting of dialysis buffer aliquots. Membrane compositions: □, 4:1:1 DA:DOH:GMD; ▲, 4:1:1 DA:DOH:GMD with 25 mol % DDPA; and *, DDPA.

changes in lipid composition that affect membrane permeability would have imposed new selective pressures. Previous work (3) has shown that the permeability of membranes composed of short-chain (C10–14) fatty acids is significantly higher than that of long-chain (C16–C18) phospholipids. However, it is unclear if this effect is because of an intrinsic physical difference between single-chain and diacyl lipid bilayers or because of the reduced bilayer thickness of short-chain lipids (23).

Here we considered the dependence of solute permeation on phospholipid content in a homogeneous C10 membrane system, as acyl chains of this length are accessible by prebiotic chemistry (10). The permeation of the sugar ribose to decanoic-acid-based membranes (4:1:1 decanoic acid:decanol:glycerol monodecanoate, DA:DOH:GMD) was strongly inhibited by increasing proportions of DDPA as measured by a real-time vesicle swelling assay (24) (Fig. 4*A*). Similarly, the permeation of 5′-imidazole-activated dAMP (ImpdA), a model prebiotic building block for template copying (25), was sixfold slower in DDPA membranes compared to monoacyl membranes (Fig. 4*B*). The increased permeability of single-chain membranes is explained by their intrinsically higher fluidity (lower order) compared to diacyl lipid membranes (Fig. 3*B*), because permeability is correlated with bilayer fluidity (26). Because this increased order also inhibits fatty acid desorption, enhanced competition proficiency is intrinsically coupled to a reduction in membrane permeability.

Discussion

The experiments presented here demonstrate that the synthesis of diacyl phospholipids would have been highly beneficial for early protocells featuring membranes composed of fatty acids and their derivatives. The chemical pathway from fatty acids to the simplest phospholipid, phosphatidic acid, occurs via successive acyl- and phosphotransfer reactions. Although the intermediates in this pathway, glycerol monoesters and lysophospholipids, stabilize fatty acid bilayers to divalent cations (15) and varying pH (27), they exchange rapidly between bilayers (28) and thus would not stay localized to a single cell. Thus, there is no selective advantage for a genomically encoded catalyst that would enable internal synthesis of these intermediates, even though an environmental source of such lipids would be beneficial. In contrast, diacyl lipids, such as phospholipids, are firmly anchored to the membrane ($t_{1/2}$ of hours to days; refs. 28 and 29) because of their decreased solubility. Therefore, the synthesis of phosphatidic acid by the acylation of a lysophospholipid with an activated fatty acid is the first step in this pathway for which a genomically encoded catalyst would confer a selective advantage. An acyltransferase ribozyme that catalyzes this reaction, analogous to the protein acyltransferases ubiquitous in phospholipid synthesis, would therefore be sufficient to drive protocell growth and could have been selected for during early cellular evolution. Once such acyltransferases had evolved, there would have been a selective advantage for the synthesis of phospholipid precursors, because they would remain associated with their host cell via incorporation into diacyl lipids.

We have argued that phospholipid-driven competition could have led early cells into an evolutionary arms race leading to steadily increasing diacyl lipid content in their membranes. We have also shown that such a transition in membrane composition would have come at the expense of membrane permeability. Cells adopting increasingly phospholipid membranes would have therefore been effectively sealing themselves off from previously available nutrients in their environment. What selective pressures would such a predicament impose on early, heterotophic cells? One possibility is that membrane transporters, a hallmark of modern cells, would have emerged as a means for overcoming low membrane permeability. Although protein channels and pumps are complex molecular assemblies, early transporters could have formed from short peptides (30) or nucleic acid assemblies (31, 32), perhaps in complexes with cationic lipids. Additionally, cells could have evolved the ability to synthesize their own building blocks from simpler, more permeable substrates (metabolism) (Fig. 5). Early catalysts, such as the phospho- and acyltransferases proposed here for phospholipid synthesis, could have been adapted for metabolic tasks such as sugar catabolism and peptide synthesis (33), respectively. The emergence of phospholipid membranes would also have allowed early cells to utilize ion gradients (30), which rapidly decay in fatty acid membranes (34), and to explore new environmental niches characterized by lower monoacyl lipid concentrations. Hence, early changes in cell membrane composition and permeability, driven by the simple physical phenomena demonstrated here, could have been an important driver of the evolution of metabolism and membrane transport machinery.

Methods

Materials. Phospholipids and diacyl glycerol were obtained from Avanti Polar Lipids. Single-chain lipids (fatty acids, fatty alcohols, and glycerol monoesters)

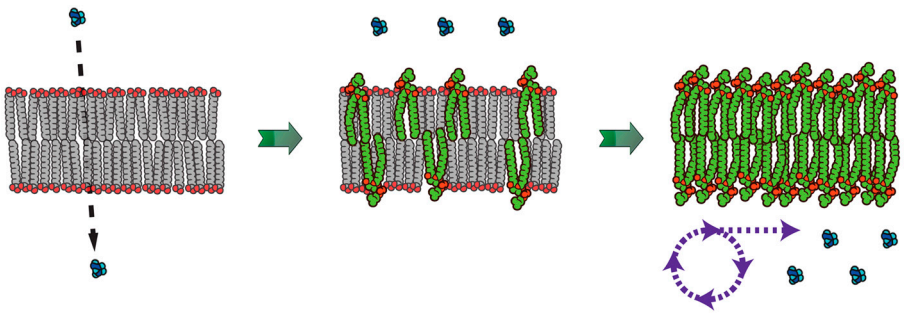

Fig. 5. Schematic for membrane-driven cellular evolution. The gradual transition from highly permeable primitive membranes (*Left*) to phospholipid membranes (*Right*) is driven by the selective growth advantage provided by increasing phospholipid content in the membrane. In turn, this transition in membrane composition imposes a selective pressure for the emergence of internalized metabolism to counter the reduced permeability of diacyl lipid membranes.

were obtained from Nu-chek Prep. Rhodamine DHPE (Rhodamine B 1,2-dihexadecanoyl-*sn*-glycero-3-phosphoethanolamine) and NBD-PE [*N*-(7-nitrobenz-2-oxa-1,3-diazol-4-yl)-1,2-dihexadecanoyl-*sn*- glycero-3-phosphoethanolamine] were obtained from Invitrogen. ^{3}H-ImpdA was prepared by activation of 2,8-^{3}H dAMP (Moravek Biochemicals) with carbonyldiimidazole (CDI) (35). Briefly, dAMP was desalted on a spin-column (Dowex, Dow Chemicals), dried, and reacted with 5 equivalents of CDI in 75:25 DMSO: dimethylformamide containing 3 equivalents of triethylamine. The imidazolide was purified by reverse-phase HPLC on a C18 column (Alltech) equilibrated with 20 mM triethylammonium bicarbonate pH 7.8, 2% acetonitrile and eluted with a 2–9% gradient of acetonitrile. All other reagents were obtained from Sigma-Aldrich.

Vesicle Preparation. Phospholipid vesicles were prepared by thin-film hydration from chloroform stock solutions. Fatty acid and mixed vesicles were prepared by dispersing the neat oil in buffer. For mixed vesicles, the phospholipid stock solution was first added to the oil and solvent evaporated. All vesicle solutions were incubated for >12 h under gentle agitation. Unilamellar vesicles were prepared by extrusion 11 times through 100-nm pore-size polycarbonate membranes in an Avanti miniextruder. All extruded vesicles were used between 4 and 24 h after extrusion. Solutes to be encapsulated were included in the hydration/dispersion buffer, and extrusion was preceded by 5–10 cycles of freeze–thaw. Unencapsulated solutes were removed by gel filtration (Sepharose-4B) or dialysis. For microscopy experiments, large, monodisperse vesicles were prepared by extrusion through 5-μm pore-size membranes followed by repeated dialysis against 3-μm pore-size membranes as previously described (4). Alternatively, for experiments using DDPA or high DOPA content, dialysis was substituted with repeated pipetting against 3-μm pore-size membranes, which act as large-pore sieves. For single-chain lipid mixtures, all gel filtration and dialysis buffers contained the appropriate lipid mixture at concentrations above the critical aggregation concentration; 100 μM for oleate mixtures and 30 mM for decanoic acid mixtures. Unless otherwise noted, vesicles were prepared in 0.2 M Na^{+}-bicine pH 8.5.

Microscopy. Vesicles to be used for imaging were prepared with 2 mM encapsulated (8-hydroxypyrene-1,3,6-trisulfonic acid (HPTS), unless otherwise noted. For competition experiments, labeled vesicles were quickly mixed with extruded, unlabeled vesicles and pipetted into a disposable hemocytometer (Incyto) or homemade flow cell for imaging. For vesicle division, shear force was applied either by blowing compressed air onto a drop of vesicle-containing solution or by gently pressing on the top of the imaging chamber. Images were taken on an inverted epifluoresence microscope (Nikon TE2000S) with extra-long working distance objective lenses. The illumination source was a metal halide lamp equipped with appropriate optical filters for fluorescence imaging and neutral density filters to minimize photobleaching. Images were recorded on a CCD camera (Hamamatsu) and processed using Phylum software. Experiments were performed at 23 °C.

Competition Measurements. The surface area of 100-nm vesicles was monitored by FRET as previously described (2, 7). Labeled vesicles were prepared with a 1:1 ratio of Rhodamine-DHPE and NBD-PE at 0.2 mol % (for oleate vesicles) or 0.4 mol % (for oleate/DOPA vesicles). For kinetic experiments, the ratio of acceptor to donor emission was recorded on a stopped-flow spectrofluorimeter (Applied Photophysics SX.18MV-R). For steady-state measurements, the FRET signal was calculated as the ratio of donor emission before and after the addition of 1% Triton X-100, measured on an in-line fluorimeter (Varian). Measurements were converted to relative surface area using standard curves of FRET signal vs. dye concentration. Total lipid concentrations were kept below 3 mM to avoid scattering artifacts. All experiments were performed in 0.2 M Na^{+}-bicine at pH 8.5, 1 mM EDTA at 23 °C.

Desorption Measurements. Fatty acid desorption rates were measured as previously described (13). Unless otherwise noted, vesicles were prepared with 0.25 mM (final concentration) of the fatty acid and were mixed with reporter vesicles (1 mM 1-palmitoyl-2-oleoyl-phosphocholine) encapsulating 0.5 mM HPTS in a stopped-flow spectrometer. The decline in the pH-sensitive HPTS emission at 510 nm (λ_{ex} 460 nm) was fitted to a first-order exponential decay. Traces were taken as the average from five independent runs. All experiments were performed in 0.2 M Na^{+}-bicine pH 8.5, 1 mM EDTA at 23 °C.

Anisotropy Measurements. DPH was added to 100-nm vesicles as a 1% vol/vol concentrated ethanol stock, followed by a >1 h incubation. Steady-state anisotropy measurements were taken as described (19) on a Cary Eclipse (Varian) spectrophotometer with a manual polarizer accessory. Anisotropy was calculated as a unitless ratio defined as $R = (I_{=} - I_{\perp})/(I_{=} + 2I_{\perp})$, where I is the emission intensity at 430 nm (λ_{ex} 360 nm) parallel ($I_{=}$) or perpendicular ($I_{\perp}$) to the direction of polarization of the excitation source. Measurements were taken at 23 °C.

Permeability Measurements. Ribose permeability was measured by the shrink–swell assay (24). Vesicles containing 10-mM encapsulated calcein were mixed with buffer containing 0.7 M ribose in a stopped-flow spectrofluorimeter. Fluorescence intensity (λ_{em} 540–560 nm, λ_{ex} 470 nm) initially declined rapidly due to water efflux, then slowly relaxed back to the initial value due to ribose (and water) influx. Solute permeability was calculated from the relaxation rate. Bicine permeability was measured similarly on an in-line fluorimeter. Nucleotide permeability was measured by monitoring leakage of 2,8-^{3}H-ImpdA from 100-nm vesicles. After encapsulation, vesicles were loaded into 65-kDa molecular-weight cutoff dialysis tubes and leakage monitored by scintillation counting of dialysis buffer aliquots (36). Except for bicine permeability, all experiments were performed in 0.1 M piperazine-1,4-bis(2-hydroxy-propanesulfonic acid) pH 8.2 at 30 °C. This buffer was chosen for its low permeability, even at elevated temperatures, which allowed us to specifically monitor ribose influx during shrink–swell experiments.

ACKNOWLEDGMENTS. We thank R. Bruckner, A. Ricardo, S. Tobé, T. Zhu, and C. Blain for discussions and S. Tobé for assistance with nucleotide permeability experiments. This work was supported by a grant from the NASA Exobiology Program (EXB02-0031-0018 to J.W.S.). J.W.S. is an Investigator of the Howard Hughes Medical Institute.

1. Hargreaves WR, Deamer DW (1978) Liposomes from ionic, single-chain amphiphiles. *Biochemistry* 17:3759–3768.
2. Hanczyz MM, Fujikawa SM, Szostak JW (2003) Experimental models of primitive cellular compartmentalization: Encapsulation, growth, and division. *Science* 302:618–622.
3. Mansy SS, et al. (2008) Template-directed synthesis of a genetic polymer in a model protocell. *Nature* 454:122–125.
4. Zhu TF, Szostak JW (2009) Coupled growth and division of model protocell membranes. *J Am Chem Soc* 131:5705–5713.
5. Haines TH (1973) Halogen- and sulfur-containing lipids of ochromonas. *Annu Rev Microbiol* 27:403–412.
6. Van Mooy BAS, et al. (2009) Phytoplankton in the ocean use non-phosphorus lipids in response to phosphorus scarcity. *Nature* 458:69–72.
7. Chen IA, Roberts RW, Szostak JW (2004) The emergence of competition between model protocells. *Science* 305:1474–1476.
8. Cheng Z, Luisi PL (2003) Coexistence and mutual competition of vesicles with different size distributions. *J Phys Chem B* 107:10940–10945.
9. Fujikawa SM, Chen IA, Szostak JW (2005) Shrink-wrap vesicles. *Langmuir* 21:12124–12129.
10. Rushdi AI, Simoneit BRT (2001) Lipid formation by aqueous Fischer-Tropsch-type synthesis over a temperature range of 100 to 400 °C. *Orig Life Evol Biosph* 31:103–118.
11. Deamer DW, Pashley RM (1989) Amphiphilic components of the Murchison carbonaceous chondrite: Surface properties and membrane formation. *Orig Life Evol Biosph* 19:21–38.
12. Simard JR, Pillai BK, Hamilton JA (2008) Fatty acid flip-flop in model membrane is faster than desorption into the aqueous phase. *Biochemistry* 47:9081–9089.
13. Zhang G, Kamp F, Hamilton JA (1996) Dissociation of long and very long chain fatty acids from phospholipid bilayers. *Biochemistry* 35:16055–16060.
14. Cistola DP, Hamilton JA, Jackson D, Small DM (1988) Ionization and phase behavior of fatty acids in water: Application of the Gibbs phase rule. *Biochemistry* 27:1881–1888.
15. Monnard PA, Apel CL, Kanavarioti A, Deamer DW (2002) Influence of ionic inorganic solutes on self-assembly and polymerization processes related to early forms of life: Implications for a prebiotic aqueous medium. *Astrobiology* 2:139–152.
16. Seelig A, Seelig J (1977) Effect of a single cis double bond on the structure of a phospholipid bilayer. *Biochemistry* 16:45–50.
17. Lund-Katz S, Laboda HM, McLean LR, Phillips MC (1988) Influence of molecular packing and phospholipid type on rates of cholesterol exchange. *Biochemistry* 27:3416–3423.
18. Silvius JR, Leventis R (1993) Spontaneous interbilayer transfer of phospholipdis: dependence on acyl chain composition. *Biochemistry* 32:13318–13326.
19. Van Blitterswijk WJ, van Hoeven RP, van der Meer BW (1981) Lipid structural order parameters (reciprocal of fluidity) in biomembranes derived from steady-state fluorescence polarization measurements. *Biochim Biophys Acta* 644:323–332.
20. Hargreaves WR, Mulvihill SJ, Deamer DW (1977) Synthesis of phospholipids and membranes in prebiotic conditions. *Nature* 266:78–80.
21. Epps DE, Sherwood E, Eichberg J, Oro J (1978) Cyanamide mediated synthesis under plausible primitive earth conditions: The synthesis of phosphatidic acids. *J Mol Evol* 11:279–292.
22. Dawkins R, Krebs JR (1979) Arms races between and within species. *Proc R Soc London Ser B* 205:489–511.
23. Paula S, Volkov AG, Van Hoek AN, Haines TH, Deamer DW (1996) Permeation of protons, potassium ions, and small polar molecules through phospholipid bilayers as a function of membrane thickness. *Biophys J* 70:339–348.

24. Sacerdote MG, Szostak JW (2005) Semipermeable lipid bilayers exhibit diastereoselectivity favoring ribose. *Proc Natl Acad Sci USA* 102:6004–6008.
25. Orgel LE (2004) Prebiotic chemistry and the origin of the RNA world. *Crit Rev Biochem Mol Biol* 39:99–123.
26. Lande MB, Donovan JM, Zeidel ML (1995) The relationship between membrane fluidity and permeabilities to water, solutes, ammonia, and protons. *J Gen Physiol* 106:67–84.
27. Apel CL, Deamer DW (2005) The formation of glycerol monodecanoate by deydration/condensation reaction: Increasing the chemical complexity of amphiphiles on the early earth. *Orig Life Evol Biosph* 35:323–332.
28. McLean LR, Phillips MC (1984) Kinetics of phosphatidylcholine and lysophosphatidylcholine exchange between unilamellar vesicles. *Biochemistry* 23:4624–4630.
29. Abreu MSC, Moreno MJ, Vaz WLC (2004) Kinetics and thermodynamics of association of a phospholipid derivative with lipid bilayers in liquid-disordered and liquid-ordered phases. *Biophys J* 87:353–365.
30. Pohorille A, Deamer D (2009) Self-assembly and function of primitive cell membranes. *Res Microbiol* 160:449–456.
31. Kaucher MS, Harrell WA, Davis JT (2006) A unimolecular G-quadruplex that functions as a synthetic transmembrane Na+ transporter. *J Am Chem Soc* 128:38–39.
32. Janas T, Janas T, Yarus M (2004) A membrane transporter for tryptophan composed of RNA. *RNA* 10:1541–1549.
33. Li N, Huang G (2005) Ribozyme-catalzyed aminoacylation from CoA thioesters. *Biochemistry* 44:4582–4590.
34. Chen IA, Szostak JW (2004) Membrane growth can generate a pH gradient in fatty acid vesicles. *Proc Natl Acad Sci USA* 101:7965–7970.
35. Hoard DE, Ott DG (1965) Conversion of mono- and oligodeoxyribonucleotides to 5′-triphosphates. *J Am Chem Soc* 87:1785–1788.
36. Chakrabarti AC, Breaker RR, Joyce GF, Deamer DW (1994) Production of RNA by a polymerase protein encapsulated within phospholipid vesicles. *J Mol Evol* 39:555–559.